

# **External Fake Constraints Interpolation: the end of Runge phenomenon with high degree polynomials relying on equispaced nodes – Application to aerial robotics motion planning**

**By Nicolas Belanger**

Airbus, Innovation Department, Marignane, France

## **Abstract**

The present paper introduces a new approximation method that suppresses the Runge phenomenon with high degree polynomials relying on equispaced nodes. The principle consists in using external constraints of the type  $P''(x)=0$  externally to the interpolation interval. As those constraints do not have any validity regarding the Runge function behavior we call them External Fake Constraints (EFC). We demonstrate that the EFC method can be of greater accuracy than Spline interpolation. We then apply the EFC principle to a simple aerial robotics motion planning problem and demonstrate the interest for linear system optimization under kinematics constraints and present the associated results. We then open the door to directions to improve and formalize EFC method and propose other applications in aerial robotics motion planning.

## **1. Introduction**

For more than a century, the Runge phenomenon [1] has fascinated generations of approximation theory mathematicians. Major advances have been made through the last two decades by researchers like J.P. Boyd [3] [4] [5] or Rodrigo Platte [6] [7] to deeply understand and defeating this counter intuitive phenomenon. Nevertheless, the general spread idea is that high order polynomial interpolation with equispaced nodes is not suitable to approximate the Runge function as demonstrated by Trefethen [2]. To mitigate the Runge problem, it is common to use the Chebyshev nodes for Lagrange interpolation which are known as the best solution to interpolate the function with polynomials while attenuating largely the wild oscillations occurring near the limits of the interpolation interval. This solution can be satisfying for mathematicians, but a lot of operational problems require the needs of equidistant nodes which is not the case with Chebyshev nodes. Thus, in order to overcome the Runge phenomenon while keeping the interest of polynomials in the solution, Dechao & al [8] explored piecewise functions such as splines. The results presented in this study are very accurate and can serve as a very good reference for the method that we aim to introduce. The authors measured the efficiency of different splines methods such as : natural cubic splines, parabolically terminated cubic splines, extrapolated cubic splines. Using the least squares error indicator :

$$E = \frac{1}{K} \sum_{k=0}^{K-1} (y_k - \hat{y}_k)^2$$

The results obtained in [8] are recapitulated in the Table 1 with  $n+1$  equidistant nodes:

| n  | Natural Cubic Spline     | Extrapolated cubic spline | Parabolically terminated cubic spline | PseudoInverse Cubic spline (PCS) |
|----|--------------------------|---------------------------|---------------------------------------|----------------------------------|
| 8  | $4.2652 \times 10^{-4}$  | $4.3859 \times 10^{-4}$   | $4.3177 \times 10^{-4}$               | $4.3132 \times 10^{-4}$          |
| 10 | $5.0729 \times 10^{-5}$  | $5.0986 \times 10^{-5}$   | $5.0623 \times 10^{-5}$               | $5.0783 \times 10^{-5}$          |
| 20 | $7.6909 \times 10^{-7}$  | $7.6857 \times 10^{-7}$   | $7.6862 \times 10^{-7}$               | $7.6879 \times 10^{-7}$          |
| 50 | $3.0750 \times 10^{-10}$ | $3.0183 \times 10^{-10}$  | $3.0193 \times 10^{-10}$              | $3.0467 \times 10^{-10}$         |

TABLE 1. Results obtained with splines interpolation in De Chao and al. [8]

Another recent work [9] based on an Immunity Genetic Algorithm (IGA) applied to a parametric curve has demonstrated that it was possible to solve the Runge phenomenon by learning methods. The results presented with the IGA method state of  $E_{error}$  of  $8.10^{-4}$  for 21 equidistant samples. The recent results obtained with the PseudoInverse Cubic Spline (PCS) interpolation [8] and with the IGA [9] will serve as a reference for our approach. In the present paper we introduce a new method which approximate the Runge function  $f(x)=1/(1+25x^2)$  within  $[-1;1]$  by the means of a single high order degree polynomial with equispaced nodes. The interest of the method goes beyond the pure mathematical exercise as we demonstrate the added value that it brings for optimization problems. We illustrate it through a case of path planning optimization for an aerial mobile robot.

## 2. External Fake Constraints Interpolation

Considering the Runge phenomenon and the wild oscillations that occur near the endpoints of the interpolation interval, we propose a new approach. Our idea is to artificially increase the degree of the initial Lagrange interpolation polynomial relying on equispaced nodes. To do so, we extend the linear system represented by  $k$  equations used to build the Lagrange interpolation polynomial with equispaced nodes. These equations which can be seen as *Lagrange interpolation contributors* in our system are of the type:

$$a_n \cdot x_{L_i}^n + a_{n-1} \cdot x_{L_i}^{n-1} + \dots + a_0 = f(x_{L_i}) \text{ (where } f \text{ is the Runge function)}$$

Where the  $x_{L_i}$  are the equidistant  $k$  nodes ( $k$  is an odd number) in the interval  $[-1;1]$

To those  $k$  equations we add  $m$  equations ( $m$  is an even number and  $k + m = n + 1$ ) that we use to stabilize the Runge phenomenon oscillations. Those  $m$  equations impose to the polynom  $P_{EFC}(x)$  that we want to find, the constraints that its second derivative is equal to 0 in  $m/2$  points located within a small interval  $]-1-\epsilon; -1]$  and  $m/2$  equations of the same type located externally and symmetrically on the interval  $[1; 1+\epsilon[$  where  $\epsilon > 0$ . We call those constraints *External Fake Constraints* (EFC) because regarding the behaviour of the second derivative of the Runge function which equation is  $f_{Runge}''(x) = \frac{5000x^2}{(25x^2 + 1)^3} - \frac{50}{(25x^2 + 1)^2}$  is never equal to 0 within the small intervals  $]-1-\epsilon; -1]$  and  $[1; 1+\epsilon[$  as it can be seen on Figure 1:

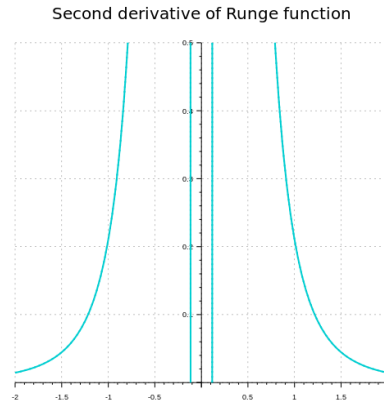


FIGURE 1. Distribution of second derivative of the Runge function

The EFC equations brought into the linear system guarantee that there will be no new oscillations generated by the increase of the interpolation polynomial degree. Indeed, introducing additional constraints on the second order derivative of the polynomial guarantee that the new oscillations due to the degree increase will be generated externally to the interval  $[-1;1]$ . So those kind of constraints are interesting because they can perform stabilization of the internal wild oscillations due to Runge phenomenon while excluding of the interpolation interval potential additional oscillations introduced by the polynomial degree increase.

Thus the global linear system that we build with the  $k+m$  equations has the following form:

$$\begin{bmatrix} x_{I_0}^n & x_{I_0}^{n-1} & x_{I_0}^{n-2} & \dots & \dots & \dots & x_{I_0} & 1 \\ x_{I_1}^n & x_{I_1}^{n-1} & x_{I_1}^{n-2} & \dots & \dots & \dots & x_{I_1} & 1 \\ \dots & \dots & \dots & \dots & \dots & \dots & \dots & \dots \\ x_{I_k}^n & x_{I_k}^{n-1} & x_{I_k}^{n-2} & \dots & \dots & \dots & x_{I_k} & 1 \\ n.(n-1).x_{EFC_1}^{n-2} & (n-1).(n-2).x_{EFC_1}^{n-3} & \dots & \dots & 6.x_{EFC_1} & 2 & 0 & 0 \\ n.(n-1).x_{EFC_2}^{n-2} & (n-1).(n-2).x_{EFC_2}^{n-3} & \dots & \dots & 6.x_{EFC_2} & 2 & 0 & 0 \\ \dots & \dots & \dots & \dots & \dots & \dots & \dots & \dots \\ n.(n-1).x_{EFC_m}^{n-2} & (n-1).(n-2).x_{EFC_m}^{n-3} & \dots & \dots & 6.x_{EFC_m} & 2 & 0 & 0 \end{bmatrix} \begin{bmatrix} a_n \\ a_{n-1} \\ \dots \\ a_1 \\ a_0 \end{bmatrix} = \begin{bmatrix} f(x_{I_0}) \\ f(x_{I_1}) \\ \dots \\ f(x_{I_k}) \\ 0 \\ 0 \\ \dots \\ 0 \end{bmatrix}$$

The challenge is then to determining  $m$  the efficient number of External Fake Constraints and

$S$  the set of abscissa positions of the fake constraints :  $S = \{ x_{EFC_1}, \dots, x_{EFC_m} \}$

The work that we performed has not yet led to a formal determination of those variables.

However the study has an empirical feature at this stage, the results we have been able to provide are of interest for future optimization problems. The linear system that we have formed is ill conditioned which does not facilitate the research of the best interpolation polynomial.

We have not explored a large range of EFC sizes and we have not explored all the possibilities in terms of  $x_{EFC_i}$  distribution over the adjacent intervals as well. That is why we think that the EFC principle still holds a big potential of improvement. We present in the following section, the results that we obtained for 5 equidistant interpolation nodes and 46 EFC points:

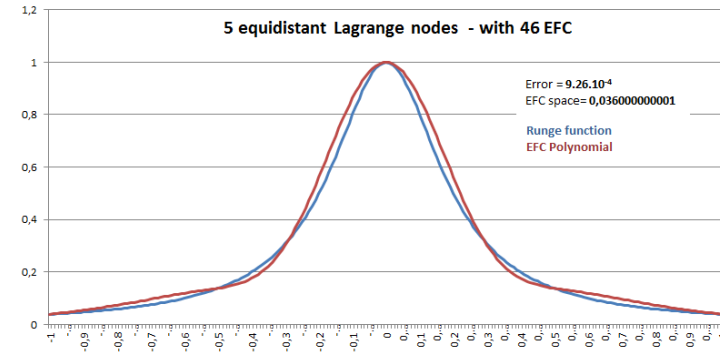


FIGURE 2. Comparison of the Runge function and EFC Interpolation for 5 equidistant nodes

The results obtained on Fig. 2 with only 5 equidistant nodes which would correspond to a degree 4 for the interpolation polynomial are quite impressive. Indeed the method allows us to reach an accuracy of  $9.26 \times 10^{-4}$  which is not that far from the results obtained by Dechao & al. [8] with the spline interpolation with 9 equidistant points. It has to be noticed that the EFC method can generate implicit crossings between the interpolation curve and the Runge function. This is the case at the abscissas -0.29 and 0.29 which are not interpolation nodes. Another remarkable point is the extreme sensitivity of the approximation to the space between

the EFC abscissas. In the presented case, the local minimum found has an increase of ten times accuracy for an extremely small variation ( $10^{-12}$ ) between the abscissa where we apply the EFC: the distance between the EFC abscissa is called the EFC space.

The results obtained for 9 equidistant nodes on Fig.3 still improve in the way of being better than the spline results as we found a local minimum at  $1.26 \times 10^{-4}$  compare to  $4.26 \times 10^{-4}$  for the spline study. We did very few attempts of varying the number of EFC so there is certainly potential to improve the accuracy of the results in the future. It has to be mentioned that the implicit EFC crossings still remain as for the 5 equidistant nodes interpolation, but the implicit crossings have lightly moved to the abscissas 0.31 and -0.31.

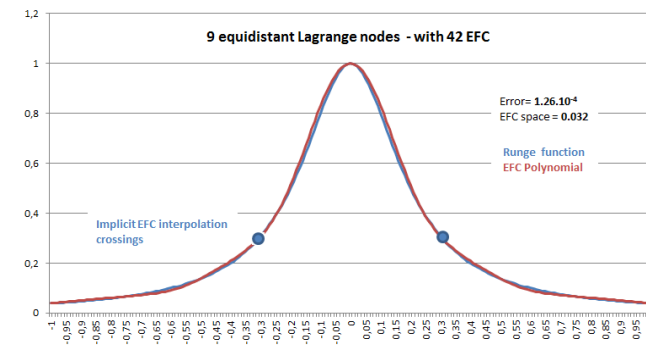


FIGURE 3. Comparison of the Runge function and EFC Interpolation for 9 equidistant nodes

The results we obtained for 11 equidistant nodes and 60 EFC on Fig.4 :  $6.21 \times 10^{-5}$  are lightly less accurate than those obtained by [8] in the spline study ( $5.06 \times 10^{-5}$ ). The explanation certainly comes from the limited tests we had with different number of EFC sets. A larger exploration of EFC sizes and their associated spaces between  $x_{EFC_i}$  should have been done to find better local minima.

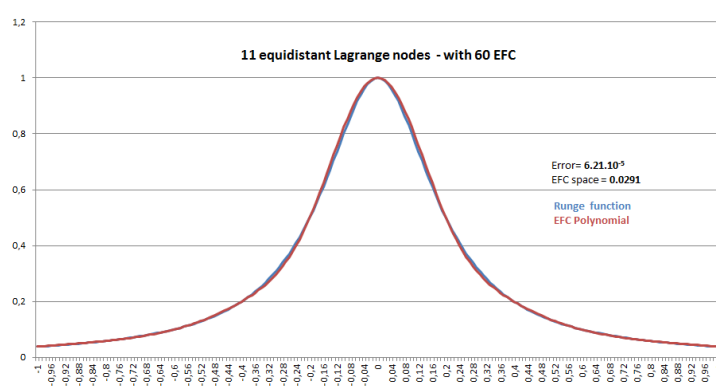


FIGURE 4. Comparison of the Runge function and EFC Interpolation for 11 equidistant nodes

At least, for 21 equidistant nodes and 50 EFC we obtain once again a better result than the one obtained with the spline approximation. Our approximation reaches  $3.41 \times 10^{-7}$  (see Figure 5.) where the spline method obtains  $7.68 \times 10^{-7}$  for the same equidistant points. The originality of the result we obtained comes from the offset of the first two  $x_{EFC_i}$  which are not positioned on the bound of the interpolation interval but slightly moved away to abscissas : 1.0073696 and -1.0073696. This result highlights another axis of improvement which deals with the potential of *non constant EFC space* (when the distance between EFC abscissa is not constant).

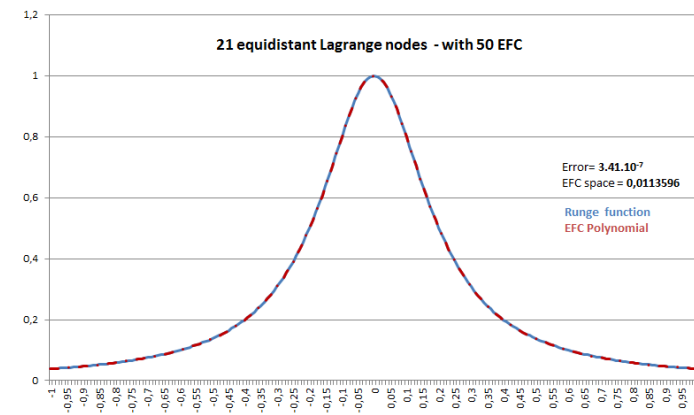


FIGURE 5. Comparison of the Runge function and EFC Interpolation for 21 equidistant nodes

Last but not least we had an attempt for the same problem with 21 equidistant nodes, to integrate few Fake Constraints of the same type  $\frac{d^2 P(x)}{dx^2} = 0$  but internally to the interpolation interval  $[-1;1]$ . With introducing those 6 internal fake constraints we obtained an accuracy of 10 times superior to spline method :  $7.10 \times 10^{-8}$ . The list of abscissas used for the fake constraints is provided in Table 2.

---

*List of abscissas used for External Fake Constraints and 6 Internal Fake Constraints (in bold)*

---

|        |       |        |              |             |              |        |        |        |        |               |              |               |        |       |
|--------|-------|--------|--------------|-------------|--------------|--------|--------|--------|--------|---------------|--------------|---------------|--------|-------|
| 1,227  | 1,214 | 1,201  | 1,188        | 1,175       | 1,162        | 1,149  | 1,136  | 1,123  | 1,11   | 1,097         | 1,084        | 1,071         | 1,058  | 1,045 |
| 1,032  | 1,019 | 1,006  | <b>0,993</b> | <b>0,98</b> | <b>0,967</b> | -1,227 | -1,214 | -1,201 | -1,188 | -1,175        | -1,162       | -1,149        | -1,136 |       |
| -1,123 | -1,11 | -1,097 | -1,084       | -1,071      | -1,058       | -1,045 | -1,032 | -1,019 | -1,006 | <b>-0,993</b> | <b>-0,98</b> | <b>-0,967</b> | -1     | 1     |

---

TABLE 2. 21 equidistant nodes – 44 EFC – 6 IFC

---

This preliminary work demonstrates the interest of managing the variations of a polynomial on a domain by the use of external constraints. The interest of this principle has been validated on a famous example : the Runge phenomenon which has been fixed. We illustrate the interest of the method for motion planning applications in aerial robotics.

### 3. Application of External Fake Constraints to aerial mobile robotics for motion planning optimization

We introduce here a simple aerial robotics motion planning problem. The idea is to generate a lateral change in a horizontal plane with a small UAV. The trajectory generation is performed by the use of a polynomial  $P(x)$ . The constraints imposed at the point  $M_s$  start of the trajectory and at  $M_f$  end of the trajectory are simple, they are expressed in a referential linked to the initial position and direction. The linear system to be solved is the following:

$$\begin{aligned}
 P(x_s) &= 0 & P(x_f) &= y_f \\
 P'(x_s) &= 0 & P'(x_f) &= 0 \\
 P''(x_s) &= 0 & P''(x_f) &= 0 \text{ (curvature=0)}
 \end{aligned} \tag{1}$$

23 November 2017, The Royal Military Academy Sandhurst, Camberley, UK

Regarding the kinematics model that we established for the UAV, at a constant speed of 120 km/h we limit the curvature of the trajectory at  $K_{\max} < 7 \times 10^{-3} \text{ m}^{-1}$ ,

calculated from :  $K(x) = \frac{y''(x)}{(1 + y'^2(x))^{\frac{3}{2}}}$ , the maximum derivative of the curvature at

$\frac{dK}{dt}_{\max} < 6.5 \times 10^{-3} \text{ m}^{-1} \text{ s}^{-1}$  and  $\frac{dK}{dt}(0) < 5 \times 10^{-3}$  at the beginning of the trajectory.

With 6 constraints to fulfil, it is required a 5 degree polynomial:

$$P(x) = a_5 x^5 + a_4 x^4 + a_3 x^3 + a_2 x^2 + a_1 x + a_0$$

And with coordinates for the ending point  $M_f(200;40)$ , solving the linear system (1) brings up the following solution :

$$a_5 = 7.5 \times 10^{-10}; a_4 = -3.75 \times 10^{-7}; a_3 = 5 \times 10^{-5}; a_2 = 0; a_1 = 0; a_0 = 0$$

We show on the Figure 6 the corresponding trajectory and its curvature distribution on Figure 7.

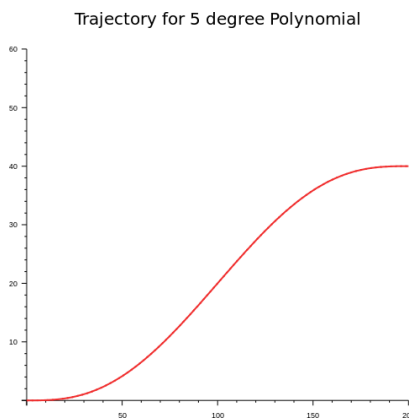


FIGURE 6. 5 degree polynomial trajectory

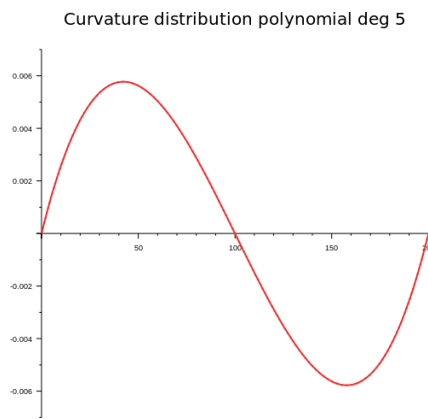


FIGURE 7. Curvature distribution for 5 degree polynomial

This is a simple solution to the problem. But with a 5 degree polynomial and 6 constraints we have no latitude to optimize the trajectory. Increasing the polynomial degree to introduce new constraints on the trajectory to optimize it in a better way involves some additional oscillations risk. That is why people generally prefer piecewise methods as Spline to get rid of the oscillations problem of a single polynomial (see §1 with [8] to solve the Runge phenomenon). But the interest of the single polynomial is that the trajectory is “deeply continuous”.

Let's now introduce two External Fake Constraints of the type :  $P''(x_{\text{EFC}}) = 0$  symmetrically outside of the trajectory interval. The first interest of those constraints is that they guarantee the additional oscillations involved by the increase of the polynomial degree will be remained externally to the domain of interest, in our case :  $[0;200]$ .

**Explanation :** As oscillations are due to a change of concavity which occurs when  $f''(x) = 0$ , imposing only constraints of this type guarantee that no additional oscillations will be generated within the bounds of the interpolation interval

The second interest of introducing two EFC in the linear system is that we bring some additional latitude to optimize the trajectory in the way that positioning the EFC at different abscissa will modify the behaviour of the polynomial within the bounds that define the trajectory problem. To be convinced about this assertion we propose to solve the linear system

corresponding to 6 trajectory constraints formed in the system (1) plus two EFC. The trajectory polynomial becomes of degree 7 and the corresponding system to be solved is then:

$$\begin{aligned} P(x_s) &= 0 & P(x_f) &= y_f & P''(x_s) &= 0 & P''(x_f) &= 0 \\ P'(x_s) &= 0 & P'(x_f) &= 0 & P''(x_{EFC1}) &= 0 & P''(x_{EFC2}) &= 0 \end{aligned} \quad (2)$$

We then solve the above system with 3 different combinations of EFC to show their direct influence on the trajectory.

$$x_{EFC1} = -0.2 \quad x_{EFC2} = 200.2$$

$$\text{Polynomial coefficients: } a_7 = -6.20651 \times 10^{-14}; \quad a_6 = 4.34456 \times 10^{-11}; \quad a_5 = -1.04217 \times 10^{-8} \\ a_4 = 8.66302 \times 10^{-7}; \quad a_3 = 3.47912 \times 10^{-7}$$

$$x_{EFC1} = -20 \quad x_{EFC2} = 220$$

$$\text{Polynomial coefficients: } a_7 = -3.53107 \times 10^{-14}; \quad a_6 = 2.47175 \times 10^{-11}; \quad a_5 = -5.60593 \times 10^{-9}; \quad a_4 = 3.31215 \times 10^{-7}; \quad a_3 = 2.17514 \times 10^{-5}$$

$$x_{EFC1} = -200 \quad x_{EFC2} = 400$$

$$\text{Polynomial coefficients: } a_7 = -4.16667 \times 10^{-15}; \quad a_6 = 2.91667 \times 10^{-12}; \quad a_5 = 0; \quad a_4 = -2.91667 \times 10^{-7}; \quad a_3 = 4.66667 \times 10^{-5}$$

Those three 7 degree polynomials are plotted on the Figure 8. It is shown the influence of the EFC positioning in the trajectory generation. We can observe on the graph that positioning the EFC next to the bounds of the trajectory interval (cyan curve) slows down the beginning and the end of the curve to capture imposed conditions in  $M_f$ . On the other side, positioning the EFC far from the bounds of the trajectory interval brings the 7 degree polynomial (red curve) next to the 5 degree polynomial.

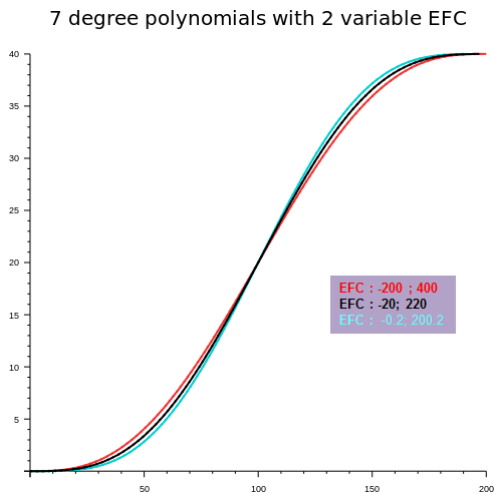


FIGURE 8. 7 degree polynomials with different EFC

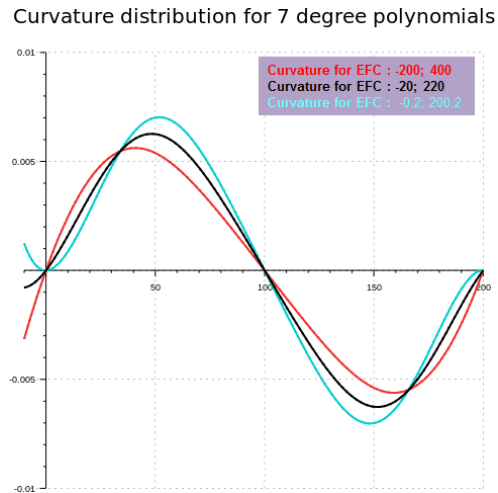


FIGURE 9. Curvature distribution for 7 degree polynomials

We can analyse the matching of the trajectory constraints on the Figure 9 where the curvature distribution is plotted for the three curves. This graph shows that when the EFC are close to

the bounds (cyan curve) the derivative of the curvature  $\frac{dK}{dx}(0)$  is close to 0 and the

maximum of the curvature is the highest of the three curves; in the present problem this constraint is slightly exceeded ( $>7.10^{-3} \text{ m}^{-1}$ ). At the same time the derivative of the curvature exceeds the maximum authorized ( $>6.5. 10^{-3} \text{ m}^{-1} \text{ s}^{-1}$ ). It comes that we cannot select this curve as a possible curve to fulfil the constraints on the trajectory. In the Table 3. We mention the other main variables for the different EFC polynomials and the 5 degree polynomial. The derivative of the curvature is calculated analytically following the below equation:

$$\frac{dK}{dt} = \frac{dK}{dx} \cdot \frac{dx}{dt} = \frac{dK}{dx} \cdot v \cdot \cos \theta = \frac{dK}{dx} \cdot v \cdot \cos(A \tan(y'(x)))$$

|                        | EFC -200; 400         | EFC -20; 220          | EFC -0.2; 200.2       | Poly. Deg 5           |
|------------------------|-----------------------|-----------------------|-----------------------|-----------------------|
| $K_{\max}$             | $5.61 \times 10^{-3}$ | $6.26 \times 10^{-3}$ | $7.02 \times 10^{-3}$ | $5.77 \times 10^{-3}$ |
| $\frac{dK}{dt}_{\max}$ | $9.33 \times 10^{-3}$ | $6.11 \times 10^{-3}$ | $6.94 \times 10^{-3}$ | $9.99 \times 10^{-3}$ |
| $\frac{dK}{dt}(0)$     | $9.33 \times 10^{-3}$ | $4.35 \times 10^{-3}$ | $7.30 \times 10^{-5}$ | $9.99 \times 10^{-3}$ |
| dS                     | 205.61 m              | 205.96 m              | 206.31 m              | 205.57 m              |

TABLE 3. Values of different main variables for EFC polynomials

As we can see in the Table 3, 5 degree polynomial and 7 degree polynomial with EFC (-200;400) largely exceed the constraints on the derivative of the curvature especially at the beginning of the trajectory. In our case the only possible solution is the 7 degree polynomial with EFC (-20;220) despite none of the constraints are saturated. For sure the above solutions are close one to the other (see close curvilinear abscissas values dS) but our goal was to point out the fact that motion planning can be managed differently by the use of EFC which is something new. Increasing the number of EFC is possible and offers new possibilities to fulfill the constraints imposed to the trajectory. We can imagine extending the principle to parametric curves by imposing constraints to negative time  $t < 0$  or time over the limit of trajectory  $t > t_{\text{limit}}$  to manage the motion planning in a better way providing more flexibility to the optimization.

#### 4. Conclusion

We introduced in the present work a new approximation method based on External Fake Constraints and high degree polynomial interpolation to solve the famous Runge phenomenon raised in 1901 by the mathematician. The EFC used in our work imposed second derivative of the polynomials to be 0. We compared our EFC method with Spline piecewise method. It has demonstrated that we were able to reach very good approximation with few equispaced nodes (5 points) which was not feasible with Spline interpolation. Until 21 equispaced nodes we had globally better results than the Spline method. Setting up few internal fake constraints immediately increase the accuracy of the method by 10 times on the computations done for 21 equispaced nodes ( $10^{-8}$  accuracy) and this result can be discussed. Anyway there is a lot of work ahead to establish a real formal EFC interpolation method as several questions have to be investigated: influence of the number of EFC, space between EFC nodes to be analyzed and mastered: constant or variable EFC space, other types of EFC like direct external constraints of  $C^0$  or  $C^1$  types which is possible but their domain of use has to be formalized analytically to avoid undesirable oscillations, mixing up EFC and IFC of  $C^2$  types. Last but not least, the system is strongly ill-conditioned and this numerical instability is certainly a major difficulty if not a limitation to approximating complex functions. But this principle can have a rich range of applications like: numerical integration, polynomial regression, Spline approximation methods improvement and motion planning optimization. On this last

application, we demonstrated on a simple case how the EFC can help to optimize the trajectory in terms of constraints fulfilment. A particular domain of interest for EFC method is certainly motion planning problems using approaches with parametric curves having polynomial curvature like of the form:  $k(s) = a_n s^n + a_{n-1} s^{n-1} + \dots + a_1 + a_0$

## REFERENCES

- [1] C. Runge, Über empirische Funktionen und die Interpolation zwischen äquidistanten Ordinaten. Z. Math. Phys. 46:224–243, 1901
- [2] L. N. Trefethen, Journal of approximation theory 65, 247-260, 1991
- [3] J. P. Boyd, J. R. Ong, “Exponentially-convergent strategies for defeating the Runge phenomenon for the approximation of non-periodic functions, part I: single-interval schemes,” Commun. Comput. Phys., vol. 5, no. 2-4, pp. 484-497, 2009.
- [4] J. P. Boyd, “Defeating the Runge phenomenon for equispaced polynomial interpolation via Tikhonov regularization,” Appl. Math. Lett., vol.5, no. 6, pp. 57-59, 1992.
- [5] J. P. Boyd, Luis F. Alfaro, “Hermite function interpolation on a finite uniform grid: Defeating the Runge phenomenon and replacing radial basis functions” Appl. Mat. Lett., vol. 26, no. 10, pp. 995-997, 2013.
- [6] Ben Adcock and Rodrigo B. Platte, A Mapped Polynomial Method for High-Accuracy Approximations on Arbitrary Grids, SIAM Journal on Numerical Analysis > Volume 54, Issue 4, 2256–2281. (26 pages), 2016
- [7] Platte R., Driscoll T., Polynomials and potential theory for Gaussian radial basis functions interpolation. SIAM J. Numer. Anal. 43, pages 750 – 766., 2005
- [8] Dechao Chen, Tianjian Qiao, Hongzhou Tan, Mingming Li and Yunong Zhang, IEEE 17<sup>th</sup> International Conference on Computational Science and Engineering, 2014
- [9] Hongwei Lin, Linjie Sun, Searching globally optimal parameter sequence for defeating Runge phenomenon by immunity genetic algorithm, Applied Mathematics and Computation 264 (2015) 85–98, Elsevier, 2015